

## ORIGINAL ARTICLE

# Deletion of adipocyte prohibitin 1 exacerbates high-fat diet-induced steatosis but not liver inflammation and fibrosis

Xiaolin Wang<sup>1</sup> | Seung-Jin Kim<sup>1</sup> | Yukun Guan<sup>1</sup> | Richard Parker<sup>1</sup>  | Robim M. Rodrigues<sup>1</sup> | Dechun Feng<sup>1</sup> | Shelly C. Lu<sup>2</sup> | Bin Gao<sup>1</sup> 

<sup>1</sup>Laboratory of Liver Diseases, National Institute on Alcohol Abuse and Alcoholism, National Institutes of Health, Bethesda, Maryland, USA

<sup>2</sup>Karsh Division of Gastroenterology and Hepatology, Department of Medicine, Cedars-Sinai Medical Center, Los Angeles, California, USA

**Correspondence**

Bin Gao, Laboratory of Liver Diseases, National Institute on Alcohol Abuse and Alcoholism, National Institutes of Health, 5625 Fishers Lane, Bethesda, MD 20892, USA.

Email: [bgao@mail.nih.gov](mailto:bgao@mail.nih.gov)

**Present address**

Xiaolin Wang, Department of Infectious Diseases, Ruijin Hospital, Shanghai Jiao Tong University School of Medicine, Shanghai, China

Seung-Jin Kim, Department of Biochemistry, College of Natural Sciences, Kangwon Institute of Inclusive Technology and Global/Gangwon Innovative Biologics-Regional Leading Research Center, Kangwon National University, Chuncheon, Korea

Richard Parker, Leeds Liver Unit, St James's University Hospital, Leeds, UK

Robim M. Rodrigues, Department of In Vitro Toxicology and Dermato-Cosmetology, Faculty of Medicine and Pharmacy, Vrije Universiteit Brussel, Brussels, Belgium

**Funding information**

National Institute on Alcohol Abuse and Alcoholism, Grant/Award Number: Intramural program

**Abstract**

Adipose tissue dysfunction is closely associated with the development and progression of nonalcoholic fatty liver disease (NAFLD). Recent studies have implied an important role of prohibitin-1 (PHB1) in adipose tissue function. In the current study, we aimed to explore the function of adipocyte PHB1 in the development and progression of NAFLD. The PHB1 protein levels in adipose tissues were markedly decreased in mice fed a high-fat diet (HFD) compared to those fed a chow diet. To explore the function of adipocyte PHB1 in the progression of NAFLD, mice with adipocyte-specific (adipo) deletion of *Phb1* (*Phb1<sup>adipo-/-</sup>* mice) were generated. Notably, *Phb1<sup>adipo-/-</sup>* mice did not develop obesity but displayed severe liver steatosis under HFD feeding. Compared to HFD-fed wild-type (WT) mice, HFD-fed *Phb1<sup>adipo-/-</sup>* mice displayed dramatically lower fat mass with significantly decreased levels of total adipose tissue inflammation, including macrophage and neutrophil number as well as the expression of inflammatory mediators. To our surprise, although liver steatosis in *Phb1<sup>adipo-/-</sup>* mice was much more severe, liver inflammation and fibrosis were similar to WT mice after HFD feeding. RNA sequencing analyses revealed that the interferon pathway was markedly suppressed while the bone morphogenetic protein 2 pathway was significantly up-regulated in the liver of HFD-fed *Phb1<sup>adipo-/-</sup>* mice compared with HFD-fed WT mice. **Conclusion:** HFD-fed *Phb1<sup>adipo-/-</sup>* mice display a subtype of the lean NAFLD phenotype with severe hepatic steatosis despite low adipose mass. This subtype of the lean NAFLD phenotype has similar inflammation and fibrosis as obese NAFLD in HFD-fed WT mice; this is partially due to reduced total adipose tissue inflammation and the hepatic interferon pathway.

Xiaolin Wang and Seung-Jin Kim contributed equally as first authors to this work.

This is an open access article under the terms of the [Creative Commons Attribution-NonCommercial-NoDerivs](https://creativecommons.org/licenses/by-nc-nd/4.0/) License, which permits use and distribution in any medium, provided the original work is properly cited, the use is non-commercial and no modifications or adaptations are made.

© 2022 The Authors. *Hepatology Communications* published by Wiley Periodicals LLC on behalf of American Association for the Study of Liver Diseases. This article has been contributed to by US Government employees and their work is in the public domain in the USA.

## INTRODUCTION

Nonalcoholic fatty liver disease (NAFLD) is the leading cause of chronic liver diseases, affecting approximately 25% of the world's population.<sup>[1]</sup> It encompasses a spectrum of clinical and histologic phenotypes from simple steatosis to nonalcoholic steatohepatitis (NASH), which can progress to cirrhosis and hepatocellular carcinoma (HCC).

Accumulating evidence has revealed the central role of adipose tissue in the complex crosstalk with the liver in NAFLD pathogenesis.<sup>[2,3]</sup> Several previous studies have suggested that adipose tissue dysfunction, such as adipose tissue inflammation, especially macrophage and neutrophil infiltration, are tightly associated with the progression<sup>[4]</sup> and severity of NASH.<sup>[5]</sup> In addition, insulin resistance, adipose tissue inflammation, and adipokine release have been shown to play an important role in controlling hepatic steatosis.<sup>[2,3]</sup> However, how adipose tissue dysfunction promotes steatosis and NASH remains obscure.

Prohibitin (PHB) is a highly conserved group of proteins that are ubiquitously expressed in many cell types and are closely associated with oxidative stress and mitochondrial biology.<sup>[6]</sup> PHB1 and PHB2 are the two highly homologous subunits of the eukaryotic mitochondrial PHB complex and are involved in maintaining mitochondrial stability.<sup>[6]</sup> Hepatic PHB1 expression is down-regulated in chronic cholestatic injury<sup>[7]</sup> and in most HCC and cholangiocarcinoma.<sup>[8]</sup> Hepatocyte-specific deletion of PHB1 resulted in spontaneous liver injury, fibrosis, and HCC.<sup>[9]</sup> Mechanically, PHB1 suppresses liver tumorigenesis by down-regulating cyclin D1 expression<sup>[9]</sup> and suppressing c-MYC, MAFG, and c-MAF expression.<sup>[8]</sup> Recent studies have also identified the important roles of PHB1 in adipose tissue functions,<sup>[10–12]</sup> such as adipocyte differentiation,<sup>[13]</sup> lipid metabolism, and thermogenesis.<sup>[14]</sup> Overexpression of PHB1 in adipocytes leads to adipocyte hypertrophy and obesity.<sup>[10,15]</sup> Conversely, genetic deletion of *Phb1* in adipocytes resulted in lipodystrophy and brown adipose tissue adaptive thermogenesis defect.<sup>[14]</sup> Mechanically, PHB1 potently inhibits glucose and fatty acid oxidation in adipocytes through inhibition of pyruvate carboxylase.<sup>[11]</sup> In addition, PHB1 and annexin A2 form a complex with the fatty acid transporter CD36 in adipocytes that regulates the transportation of free fatty acids (FFAs) into adipocytes.<sup>[12]</sup> Although adipocyte PHB1 plays an important role in controlling adipocyte functions, how adipocyte PHB1 affects NAFLD development and progression remains unknown.

In the current study, we generated adipocyte-specific (adipo) *Phb1* knockout (*Phb1<sup>adipo-/-</sup>*) mice and used them to explore the roles of adipocyte PHB1 in modulating high-fat diet (HFD)-induced NAFLD. We observed *Phb1<sup>adipo-/-</sup>* mice developed much more severe liver steatosis than wild-type (WT) mice even though

only WT mice developed obesity. Interestingly, liver injury and fibrosis were comparable between HFD-fed WT and *Phb1<sup>adipo-/-</sup>* mice. RNA-sequencing (RNA-seq) analyses identified several pathways that may contribute to the more severe steatosis but similar liver injury and fibrosis in *Phb1<sup>adipo-/-</sup>* mice compared to WT mice.

## MATERIALS AND METHODS

### Mice

Adiponectin Cre mice (stock no: 028020) were purchased from the Jackson Laboratory (Bar Harbor, ME). *Phb1*-floxed mice were generated as described.<sup>[9]</sup> Homozygous *Phb1<sup>flox/flox</sup>* mice were crossed with AdipoCre mice through several steps to generate AdipoCre<sup>+</sup> *Phb1<sup>flox/flox</sup>* (*Phb1<sup>adipo-/-</sup>*) and AdipoCre<sup>-</sup> *Phb1<sup>flox/flox</sup>* littermate controls (defined as WT mice). *Phb1<sup>adipo-/-</sup>* and WT mice (male, 7–8 weeks of age) were fed an HFD (60 kcal% fat; D12492; Research Diets, New Brunswick, NJ) for 3 months and sacrificed for analyses. All animal experiments were approved by the National Institute on Alcohol Abuse and Alcoholism Animal Care and Use Committee.

### Serum analysis

Serum samples were prepared from the mouse blood at sacrifice. Serum alanine aminotransferase (ALT) levels were measured by ALT (serum glutamate pyruvate transaminase [SGPT]) Kinetic Kit (Teco Diagnostics, Anaheim, CA) according to the manufacturer's instructions. Serum leptin levels were measured by using Mouse/Rat Leptin Quantikine Enzyme-Linked Immunoassay Kit (R&D Systems, Minneapolis, MN) following the manufacturer's protocol.

### Plasma and hepatic lipid analysis

Plasma and hepatic triglyceride (TG) levels were measured using the TG Colorimetric Assay Kit (Cayman Chemical, Ann Arbor, MI) according to the manufacturer's instructions. Plasma and hepatic cholesterol were measured with the Cholesterol Fluorometric Assay Kit (Cayman Chemical) according to the manufacturer's instructions.

### Histologic and immunohistochemical analysis

Liver and adipose tissue samples were fixed in 10% formalin and then paraffin embedded following standard procedure. We subjected 4- $\mu$ m-thick paraffin

sections to staining with hematoxylin and eosin (H&E) or with sirius red dyes (Sigma, St. Louis, MO) or to immunohistochemical staining for myeloperoxidase (MPO) and F4/80 by using primary antibodies specific to MPO (Biocare Medical, Concord, CA) or F4/80 (Cell Signaling Technology, Danvers, MA).

### Quantitative reverse-transcription polymerase chain reaction

Total RNA was isolated and purified from liver tissues or adipose tissues using TRIzol reagents (Thermo Fisher, Waltham, MA) according to the manufacturer's instructions. One microgram of RNA was reverse transcribed into complementary DNA (cDNA) using the High-Capacity cDNA Reverse Transcription Kit (Thermo Fisher). Expression levels of messenger RNA (mRNA) were measured by quantitative reverse transcription polymerase chain reaction (RT-qPCR) with the ABI7500 RT-PCR system (Applied Biosystems, Foster City, CA). The 18S ribosomal RNA was used as the invariant control. The primer sequences used for PCR reactions are listed in Table S1. Results from the RT-qPCR were subjected to statistical analysis.

### Western blot analysis

Adipose tissues were homogenized in radio immunoprecipitation assay buffer containing a cocktail of protease inhibitors (Santa Cruz Biotechnology, Dallas, TX) according to the manufacturer's instructions. Protein extracts were loaded onto 12% Bis-Tris protein gels (Bio-Rad, Hercules, CA) and transferred onto nitrocellulose membranes (Thermo Fisher). Protein bands were visualized with Pierce Enhanced Chemiluminescence Western Blotting Substrate (Thermo Fisher). The antibody against  $\beta$ -actin was purchased from Abcam (Cambridge, MA). The antibody against PHB1 protein was purchased from Cell Signaling Technology.

### Complete blood count test

Anticoagulated blood was collected from mice. A complete blood count test was performed with the Hemavet 950 FS Hematology Analyzer (Drew Scientific, Dallas, TX).

### Oral glucose tolerance test

*Phb1*<sup>adipo<sup>-/-</sup></sup> and WT mice were subjected to oral glucose tolerance tests (OGTTs) following an overnight fasting, and 0.75 mg of glucose/g of body weight was delivered by oral gavage of a 25% glucose solution dissolved in

sterile saline. Blood glucose was measured by cutting the tail tips immediately before and at 15, 30, 60, 90, and 120 minutes after glucose challenge.

### RNA-seq analysis

Total RNA was extracted from whole livers using Trizol (TRZ-100; Alkali Scientific). Liver RNA-seq was performed using Illumina HiSeq at GENEWIZ (Azenta US, Inc.). Sequence reads were trimmed to remove possible adapter sequences and nucleotides with poor quality using Trimmomatic (v.0.36).<sup>[16]</sup> Trimmed reads were mapped to the *Mus musculus* GRCm38 reference genome available on ENSEMBL using Hisat2 (v2.2.0).<sup>[17]</sup> Aligned reads were counted by FeatureCounts (v2.0.0).<sup>[18]</sup> Gene raw counts were normalized, and differential expression analysis was performed with the R package DESeq2 (v1.30.1).<sup>[19]</sup> Genes with fold change >1.5 and adjusted  $p < 0.05$  were put into gene set enrichment analysis using the R package clusterProfiler (v3.18.1).<sup>[20]</sup> R package pheatmap (v1.0.12) was used to create the heatmap plots. RNA-seq data are deposited (GEO accession number: GSE 213355).

### Statistical analysis

Results are expressed as mean  $\pm$  SEM and were analyzed using GraphPad Prism (v7.0a; GraphPad Software, La Jolla, CA). Two group comparisons were performed using the unpaired  $t$  test.  $p < 0.05$  was considered significant. Data from multiple groups were compared with one-way analysis of variance followed by Tukey's post hoc test.  $p < 0.05$  was considered significant.

## RESULTS

### HFD feeding decreases PHB1 protein expression in adipose tissue

To understand the function of adipocyte PHB1 in HFD-induced fatty liver, mice were fed an HFD or chow diet for 3 months. We first examined the expression of PHB1 proteins in adipose tissue in mice under HFD or chow feeding. Western blot analysis showed that the protein expression of PHB1 was significantly decreased in the adipose tissue of HFD-fed mice compared to chow-fed mice (Figure 1A,B). Interestingly, the mRNA level of *Phb1* in adipose tissue showed an increasing trend in HFD-fed mice compared to chow-fed mice (Figure 1C), suggesting that down-regulated PHB1 protein expression is regulated at the posttranslational levels in adipose tissue. Given that obesity is accompanied with increased number and size of differentiated mature adipocytes, we further investigated whether PHB1

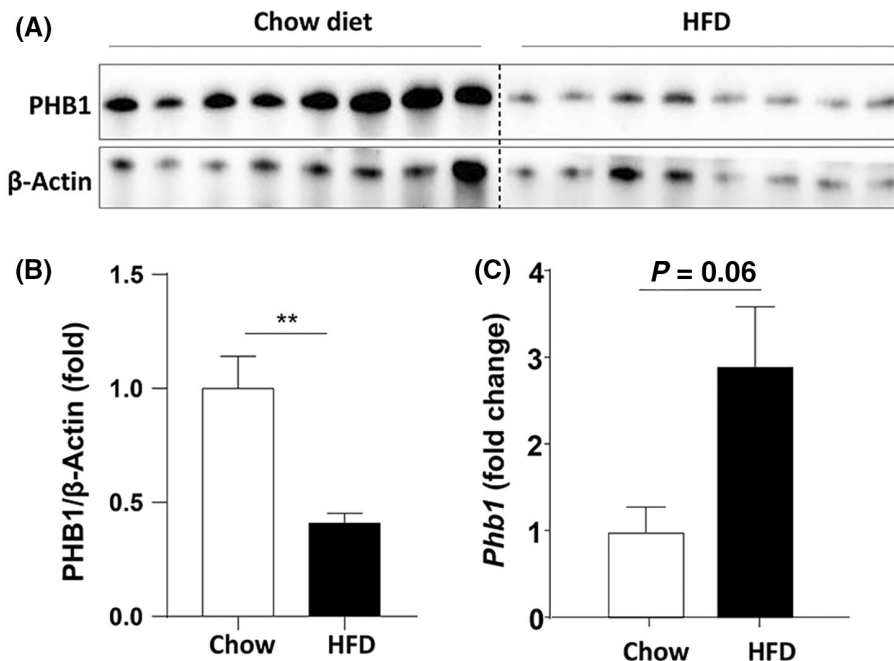


**FIGURE 1** Expression levels of PHB1 protein and *Phb1* mRNA in adipose tissues. (A,B) PHB1 protein levels in adipose tissue of mice fed a chow diet or an HFD. Protein band density quantitation is shown in panel B. (C) *Phb1* mRNA levels in adipose tissue of mice fed a chow diet or an HFD. Values represent mean  $\pm$  SEM. HFD, high-fat diet; mRNA, messenger RNA; PHB1, prohibitin-1. \*\* $p < 0.01$

was involved in the differentiation of adipocytes. We analyzed the expression of *Phb1* in 3T3L1 cells during adipocyte differentiation. mRNA levels of *Phb1* were increased in differentiated 3T3L1 cells compared to those in preadipocytes, as illustrated in Figure S1A.

### Adipocyte *Phb1* deletion leads to reduced adipose tissue mass, reduced total adipose inflammation, and adipose dysfunction after HFD feeding

Given that adipose tissue plays an essential role in the pathogenesis of fatty liver diseases, we further investigated the roles of adipocyte PHB1 in the progression of fatty liver by using *Phb1*<sup>adipo<sup>-/-</sup></sup> mice (confirmed genotyping in Figure S1B). *Phb1* deletion was confirmed by significantly reduced mRNA levels of *Phb1* in the adipose tissue of *Phb1*<sup>adipo<sup>-/-</sup></sup> mice (Figure S1C). PHB1 has been shown to play an important role in controlling adipocyte differentiation and function,<sup>[14]</sup> but how adipocyte PHB1 affects NAFLD remains obscure. To answer this question, we fed WT and *Phb1*<sup>adipo<sup>-/-</sup></sup> mice an HFD diet for 3 months. *Phb1*<sup>adipo<sup>-/-</sup></sup> mice were resistant to HFD-induced weight gain (Figure 2A). Moreover, the OGTT showed improved glucose tolerance in *Phb1*<sup>adipo<sup>-/-</sup></sup> mice under the HFD (Figure S2). In addition, we observed dramatically decreased size and weight of epididymal white adipose tissue (WAT), subcutaneous WAT, renal WAT, and brown adipose tissue in *Phb1*<sup>adipo<sup>-/-</sup></sup> mice compared with WT mice (Figure 2B,C). Histochemical staining analysis of

epididymal WAT revealed the decreased size of adipose tissue in *Phb1*<sup>adipo<sup>-/-</sup></sup> mice compared to that in WT mice (Figure S3A). Serum leptin levels were highly elevated in WT mice after HFD feeding, but such elevation was blunted in *Phb1*<sup>adipo<sup>-/-</sup></sup> mice (Figure 2D); this is consistent with the reduced fat mass in *Phb1*<sup>adipo<sup>-/-</sup></sup> mice compared with WT mice under an HFD (Figure 2B,C). Serum levels of TG and cholesterol were comparable between WT and *Phb1*<sup>adipo<sup>-/-</sup></sup> mice under HFD feeding (Figure 2E).

Interestingly, adipose fibrosis was found in WAT from *Phb1*<sup>adipo<sup>-/-</sup></sup> mice under chow or HFD feeding; this was more severe in *Phb1*<sup>adipo<sup>-/-</sup></sup> mice than in WT mice (Figure 3A,B). Consistent with adipose tissue dystrophy, genes responsible for lipid droplet formation, such as diacylglycerol o-acyltransferase 1 (*Dgat1*) and perilipin 1 (*Plin1*), were down-regulated in *Phb1*<sup>adipo<sup>-/-</sup></sup> mice compared with WT mice (Figure 3C, graphs on left). The expression of genes responsible for TG synthesis, such as peroxisome proliferator-activated receptor gamma (*Pparg*) and sterol-regulatory element binding protein 1C (*Srebp1c*), was comparable between WT and *Phb1*<sup>adipo<sup>-/-</sup></sup> mice (Figure S3B). Interestingly, expression levels of genes responsible for lipolysis, such as hormone-sensitive lipase (*Hsl*) and adipose TG lipase (*Atgl*), were also down-regulated in *Phb1*<sup>adipo<sup>-/-</sup></sup> mice compared with WT mice, which might be a compensation mechanism to maintain adipose tissue mass in *Phb1*<sup>adipo<sup>-/-</sup></sup> mice (Figure 3C, graphs on right).

Histochemical staining analysis of epididymal WAT revealed a similar infiltration of macrophages and neutrophils under both the chow diet and the HFD

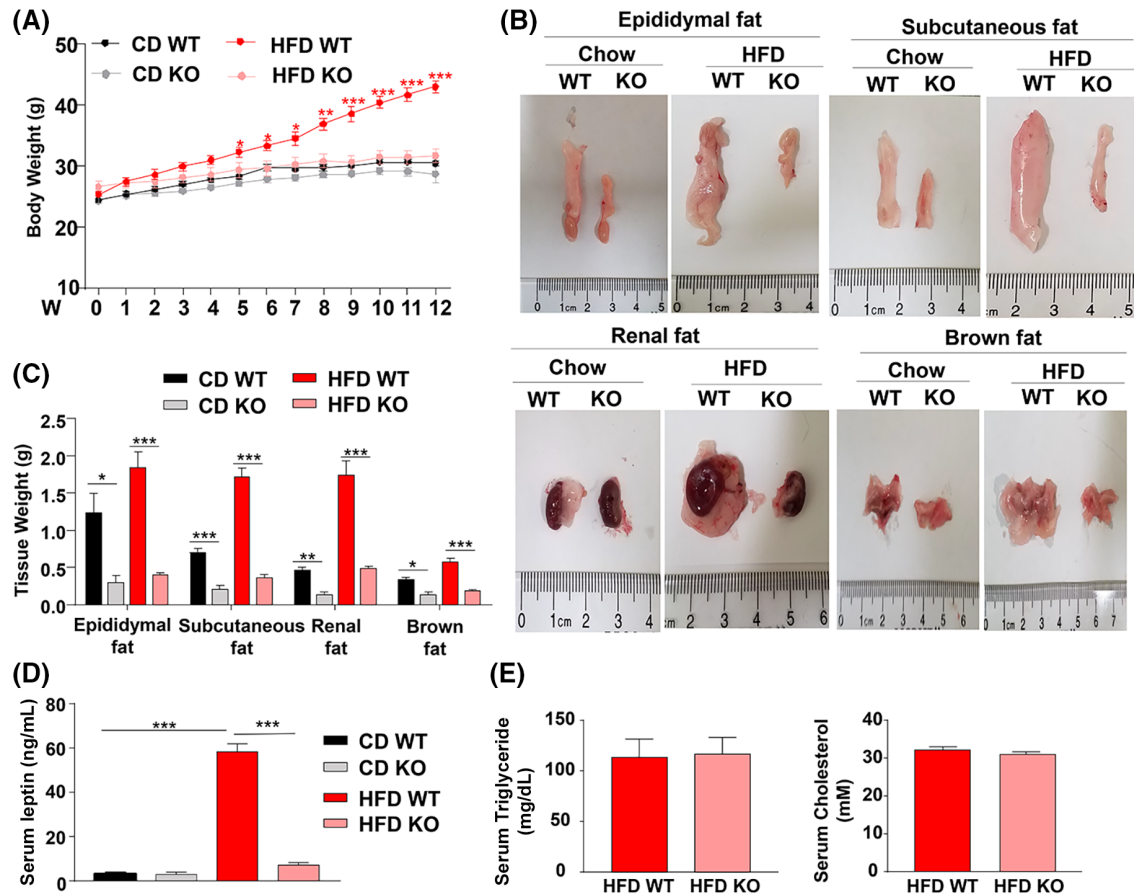


**FIGURE 2** Adipocyte-specific deletion of *Phb1* reduces adipose tissue mass. (A) WT and KO (*Phb1*<sup>adipo<sup>-/-</sup>) mice were fed a chow diet or an HFD for 3 months, and body weight of mice was recorded. (B,C) The weights of different adipose tissues were assessed at sacrifice. (D) Serum levels of leptin were measured. (E) Serum levels of triglyceride and cholesterol in WT and KO mice under an HFD. Values represent mean  $\pm$  SEM. adipo, adipocyte specific; CD, chow diet; HFD, high-fat diet; KO, knockout; PHB1, prohibitin-1; W, week; WT, wild type. \* $p < 0.05$ ; \*\* $p < 0.01$ ; \*\*\* $p < 0.001$</sup>

(Figure 4A). The infiltrated macrophages and neutrophils in adipose tissue were identified by F4/80 and MPO staining, respectively (Figure 4A). The relative numbers of macrophages (Figure 4B) and neutrophils (Figure 4C) were analyzed by quantifying the positive area for F4/80 and MPO staining, respectively. Notably, the relative numbers of macrophages and neutrophils per field were comparable in the adipose tissue of WT and *Phb1*<sup>adipo<sup>-/-</sup> mice (Figure 4B,C, graphs on left). Because the fat mass was markedly reduced in *Phb1*<sup>adipo<sup>-/-</sup> mice, further analysis showed that the relative numbers of macrophages and neutrophils in total adipose tissue were dramatically reduced in the adipose tissue of *Phb1*<sup>adipo<sup>-/-</sup> mice compared to those in WT mice (Figure 4B,C, graphs on right). Furthermore, analysis of genes corresponding to inflammatory mediators in adipose tissue per the same mRNA loading showed comparable expression levels between WT and *Phb1*<sup>adipo<sup>-/-</sup> mice (Figure 4D), while the relative expressions of these genes in total adipose tissues was accordingly much lower in HFD-fed *Phb1*<sup>adipo<sup>-/-</sup> mice compared to HFD-fed WT mice because of the much smaller fat mass in *Phb1*<sup>adipo<sup>-/-</sup> mice compared to WT</sup></sup></sup></sup></sup></sup>

mice (data not shown). These results suggest that adipocyte *Phb1* deletion leads to reduced total adipose inflammation after HFD feeding.

### Adipocyte *Phb1* deletion leads to severe liver steatosis

Given that adipose tissue dysfunction is closely associated with the development and progression of NAFLD,<sup>[4,5]</sup> we further determined the effects of adipocyte *Phb1* deletion in the HFD-induced fatty liver. We compared the liver weight and TG content of WT and *Phb1*<sup>adipo<sup>-/-</sup> mice under both the chow diet and the HFD. Liver weight and total TG in the whole liver were significantly higher in *Phb1*<sup>adipo<sup>-/-</sup> mice than in WT mice (Figure 5A,B). H&E staining analyses further revealed increased lipid accumulation in *Phb1*<sup>adipo<sup>-/-</sup> mouse liver compared with that in WT mice (Figure 5C,D). Cholesterol levels in the whole livers were comparable between WT and *Phb1*<sup>adipo<sup>-/-</sup> mice under the HFD (Figure S4). Analysis of genes involved in lipid metabolism showed higher mRNA levels of stearoyl-coenzyme</sup></sup></sup></sup>

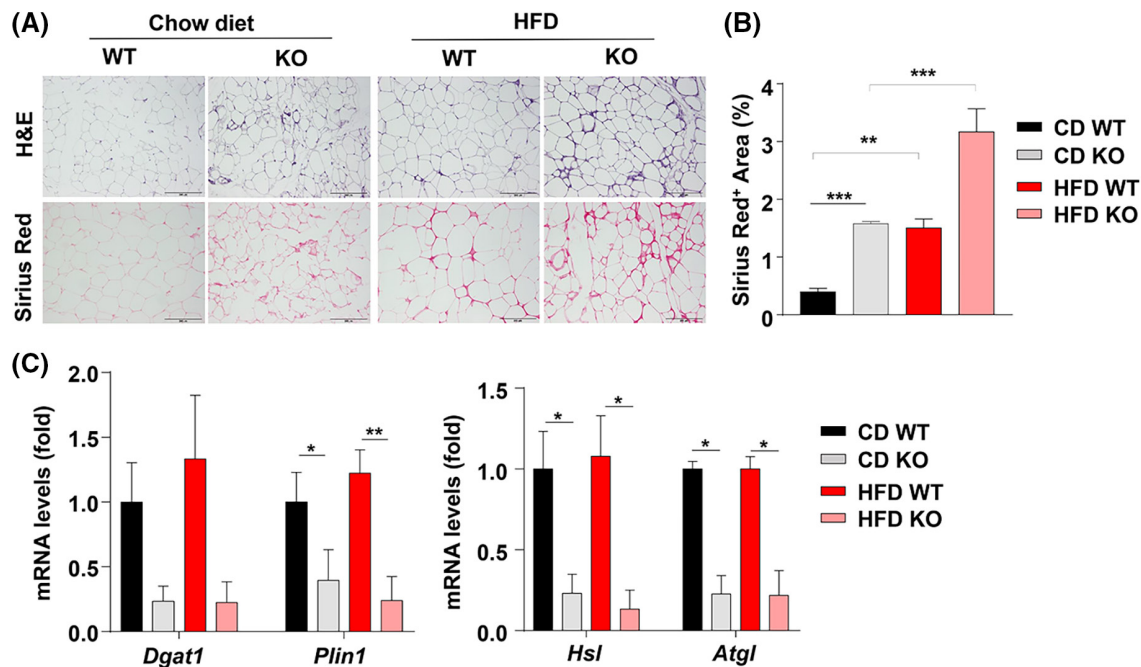


**FIGURE 3** *Phb1*<sup>adipo-/-</sup> mice display abnormal adipose tissue morphology and function. (A) Representative micrographs of adipose tissue sections subjected to H&E and sirius red staining (scale bars, 200  $\mu$ m). (B) Areas positive for sirius red staining in adipose tissue were quantified. (C) Quantitative reverse-transcription polymerase chain reaction analyses of the genes responsible for lipid droplet formation and lipolysis in epididymal white adipose tissue. Values represent mean  $\pm$  SEM. *adipo*, adipocyte specific; *Atgl*, adipose triglyceride lipase; CD, chow diet; *Dgat1*, diacylglycerol o-acyltransferase 1; H&E, hematoxylin and eosin; HFD, high-fat diet; *Hsl*, hormone-sensitive lipase; KO, knockout; mRNA, messenger RNA; PHB1, prohibitin-1; *Plin1*, perilipin 1; WT, wild type. \* $p < 0.05$ ; \*\* $p < 0.01$ ; \*\*\* $p < 0.001$

A (CoA) desaturase-1 (*Scd1*) and *Cd36* in *Phb1*<sup>adipo-/-</sup> mice than those in WT mice under a chow diet while lower mRNA levels of *Ppara*, fatty acid binding protein 1 (*Fabp1*), and *Fabp5* in *Phb1*<sup>adipo-/-</sup> mice than those in WT mice under the HFD (Figure 5E).

### Liver inflammation and fibrosis were comparable between WT and *Phb1*<sup>adipo-/-</sup> mice under the HFD

Severe liver steatosis always leads to increased liver inflammation; thus, we further investigated liver injury, inflammation, and fibrosis in *Phb1*<sup>adipo-/-</sup> mice. To our surprise, serum ALT levels were comparable between WT and *Phb1*<sup>adipo-/-</sup> mice under both the chow diet and HFD (Figure 6A). Intrahepatic macrophage and neutrophil infiltration as well as liver fibrosis were also similar between WT and *Phb1*<sup>adipo-/-</sup> mice under the HFD, as evidenced by F4/80, MPO, and sirius red staining (Figure 6B). In agreement with a similar number of MPO<sup>+</sup> neutrophils in the liver between WT and *Phb1*<sup>adipo-/-</sup> mice, serum levels of neutrophil-recruiting chemokine C-X-C motif chemokine ligand 1 (CXCL1) were comparable between these two groups (Figure 6C). We further analyzed genes involved in liver inflammation and fibrosis by RT-qPCR (Figure 6D). Our results showed that hepatic *F4/80* levels were lower in *Phb1*<sup>adipo-/-</sup> mice compared with WT mice under HFD

or chow diet feeding. Hepatic interleukin 6 (*Il6*) levels were also lower in *Phb1*<sup>adipo-/-</sup> mice compared with WT mice under chow diet feeding (Figure 6D, graphs on left), suggesting liver inflammation is not enhanced in *Phb1*<sup>adipo-/-</sup> mice despite enhanced steatosis compared to WT mice. Interestingly, hepatic expression of several genes responsible for liver fibrosis did not show a significant difference between WT and *Phb1*<sup>adipo-/-</sup> mice (Figure 6D, graphs on right). Hepatic mRNA levels of actin alpha 2, smooth muscle (*Acta2*) showed an increasing trend while the mRNA levels of collagen type I alpha 2 (*Col1a2*) and *Col3a1* tended to decrease in *Phb1*<sup>adipo-/-</sup> mice compared to WT mice under the HFD, as illustrated in Figure 6D. However, these differences were not statistically significant.

### The NAFLD phenotype in *Phb1*<sup>adipo-/-</sup> mice is associated with dysregulation of the interferon and bone morphogenetic protein 2 pathways

The above-mentioned interesting results prompted us to investigate the molecular mechanisms underlying the greater severity of steatosis, notwithstanding similar inflammation and fibrosis in *Phb1*<sup>adipo-/-</sup> mice compared to WT mice. To this end, we performed RNA-seq analyses of liver tissues from WT and *Phb1*<sup>adipo-/-</sup> mice under HFD feeding. A volcano plot of RNA-seq data

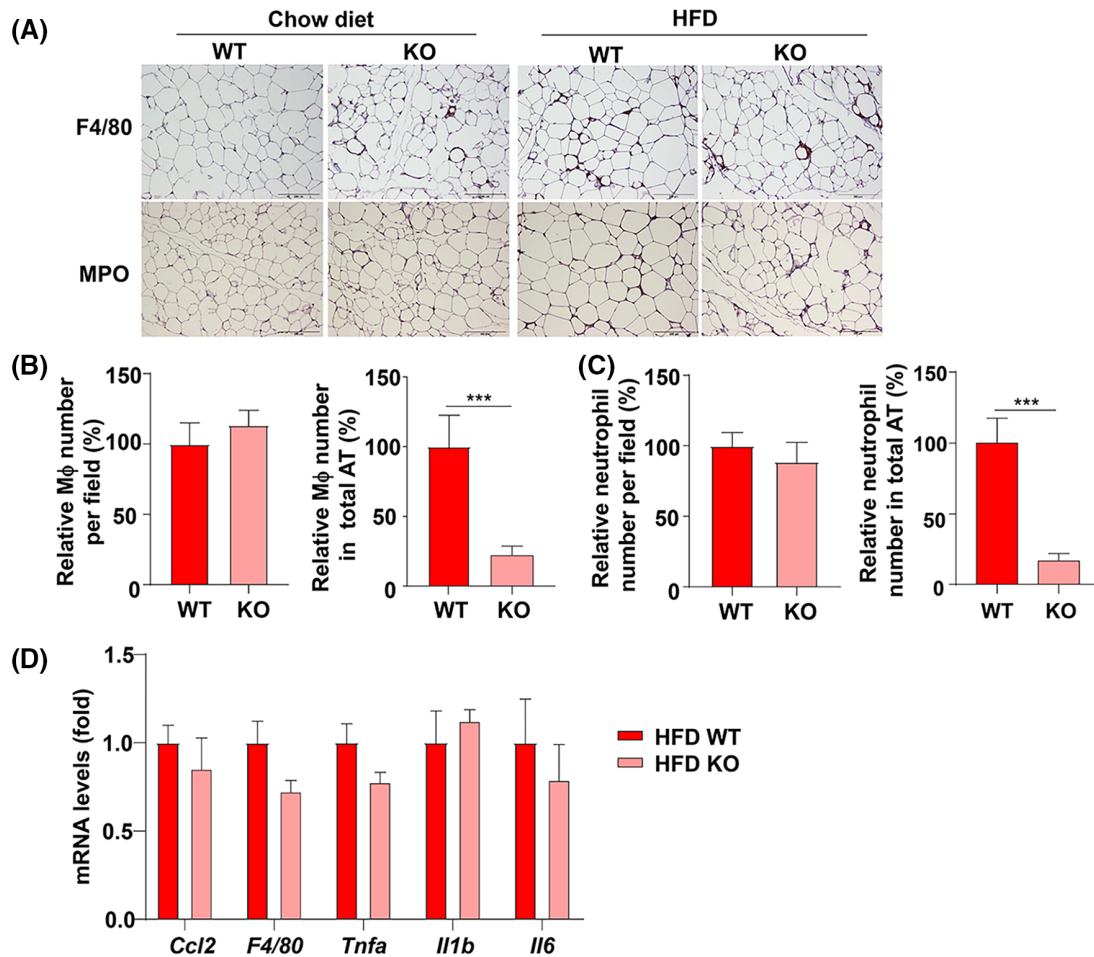


**FIGURE 4** HFD-induced adipose tissue inflammation is much lower in *Phb1<sup>adipo-/-</sup>* mice than in WT mice. (A) Representative micrographs of adipose tissue sections subjected to F4/80 and MPO staining (scale bars, 200  $\mu$ m). (B,C) Relative numbers of macrophages and neutrophils in adipose tissue. The positive area for F4/80 (representing macrophages) and MPO (representing neutrophils) staining in the paraffin-embedded adipose tissue sections were quantified, and the corresponding relative numbers of macrophages and neutrophils per field were determined. The relative numbers of macrophages and neutrophils in total adipose tissue were further calculated by multiplying adipose tissue weight. (D) Epididymal white adipose tissues were subjected to quantitative reverse-transcription polymerase chain reaction analyses of the genes related to inflammation. Values represent mean  $\pm$  SEM. *adipo*, adipocyte specific; *Ccl2*, C-C motif chemokine ligand 2; HFD, high-fat diet; *Il*, interleukin; KO, knockout; M $\phi$ , macrophage; MPO, myeloperoxidase; mRNA, messenger RNA; PHB1, prohibitin-1; *Tnfa*, tumor necrosis factor  $\alpha$ ; WT, wild type. \*\*\* $p$  < 0.001

was created to visualize the genes that were significantly altered in the livers between HFD-fed WT and *Phb1<sup>adipo-/-</sup>* mice (Figure 7A). We observed that the expression of serine (or cysteine) peptidase inhibitor, clade A, member 3C (*Serpina3c*) was dramatically up-regulated in *Phb1<sup>adipo-/-</sup>* mice compared with that in WT mice under the HFD. Given *Serpina3* is up-regulated in activated hepatic stellate cells (HSCs) compared with quiescent HSCs,<sup>[21]</sup> our data suggest a potential higher responsiveness of *Phb1<sup>adipo-/-</sup>* mice to recurrent profibrogenic stimulation compared to WT mice. Hepatic expression of cell death-inducing DFFA like effector A (*Cidea*) was greater in HFD-fed *Phb1<sup>adipo-/-</sup>* mice compared with HFD-fed WT mice. Furthermore, acyl-CoA thioesterase 3 (*Acot3*) was markedly decreased in *Phb1<sup>adipo-/-</sup>* mice compared with WT mice. CIDEA has been shown to promote steatosis by acting as an

important sensor of dietary FFAs to mediate saturated FFA-induced very low-density lipoprotein lipidation and lipid accumulation,<sup>[22]</sup> and ACOT3 is a PPAR $\alpha$  target and catalyzes the hydrolysis of acyl-CoA esters to produce FFA and CoA.<sup>[23]</sup> Thus, we speculated that the increased expression of *Cidea* and decreased expression of *Acot3* may be responsible for the severe liver steatosis in *Phb1<sup>adipo-/-</sup>* mice under the HFD.

Next, we performed gene set enrichment analysis (GSEA) and evaluated hallmark gene sets. As illustrated by GSEA and heatmap analysis, we observed that the interferon (IFN)- $\alpha/\gamma$  response pathways were markedly down-regulated in *Phb1<sup>adipo-/-</sup>* mice compared with WT mice (Figure 7B), while bone morphogenetic protein 2 (BMP2)-target genes were up-regulated in *Phb1<sup>adipo-/-</sup>* mice compared with WT mice (Figure 7C). Given the important role of the IFN and BMP2 pathways in

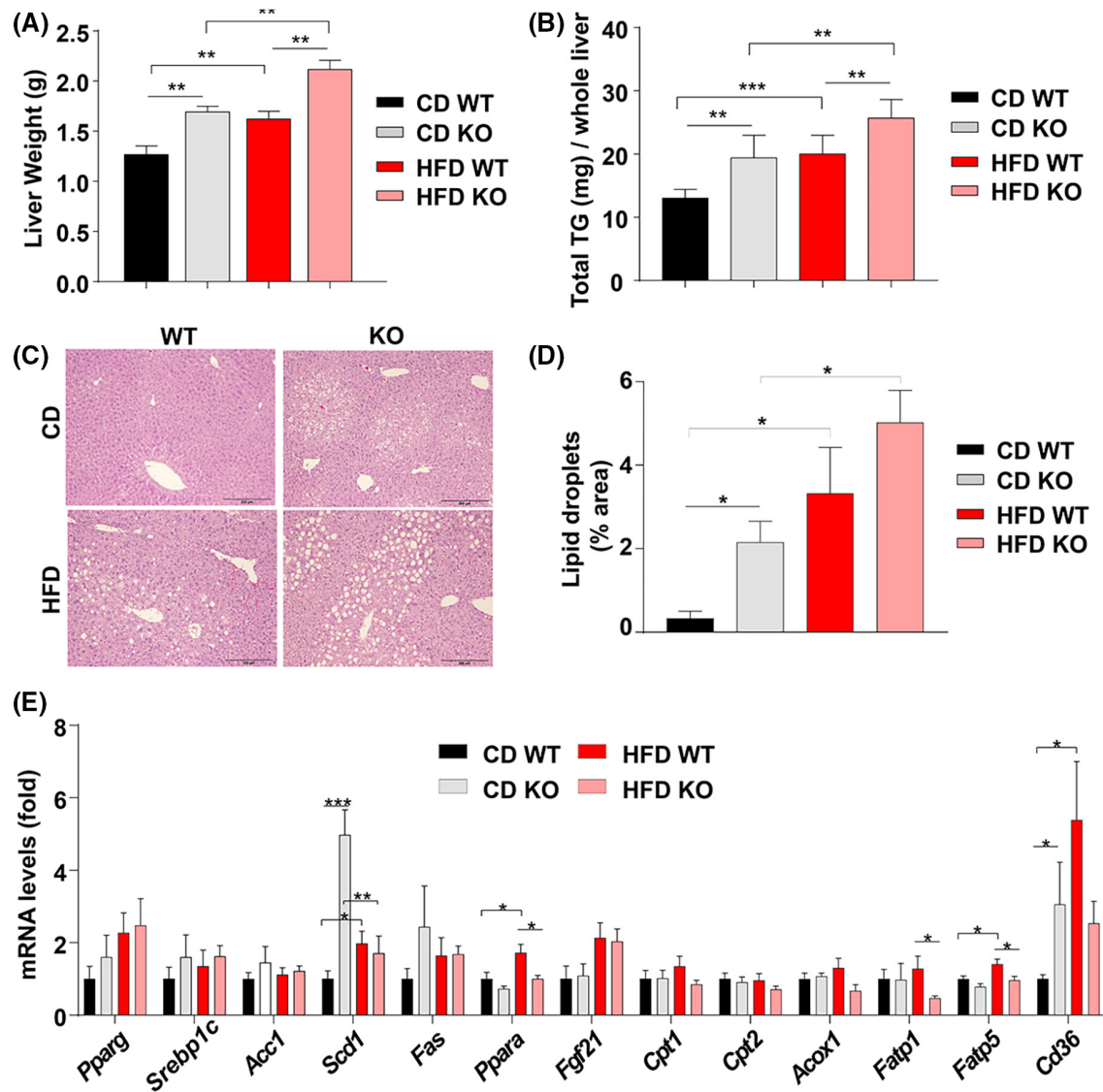


**FIGURE 5** HFD-induced steatosis is more severe in *Phb1<sup>adipo-/-</sup>* mice than WT mice. WT and *Phb1<sup>adipo-/-</sup>* mice were fed a chow diet or an HFD for 3 months. (A) Liver weight of mice was measured at sacrifice. (B) Total triglyceride levels in liver tissues. (C) Hematoxylin and eosin staining of liver sections (scale bars, 200  $\mu$ m). (D) Lipid droplets in liver tissue were quantified. (E) Quantitative reverse-transcription polymerase chain reaction analyses of hepatic genes related to lipid metabolism in liver tissues of WT and *Phb1<sup>adipo-/-</sup>* mice. Values represent mean  $\pm$  SEM. Acc1, acetyl-coenzyme A carboxylase 1; Acox1, acyl-coenzyme A oxidase 1; adipo, adipocyte specific; CD, chow diet; Cpt, carnitine palmitoyltransferase; Fas, fatty acid synthase; Fatp, fatty acid transport protein; Fgf21, fibroblast growth factor 21; HFD, high-fat diet; KO, knockout; mRNA, messenger RNA; PHB1, prohibitin-1; Ppar, peroxisome proliferator-activated receptor; Scd1, stearoyl-coenzyme A desaturase-1; Srebp1c, sterol-regulatory element binding protein 1C; TG, triglyceride; WT, wild type. \* $p < 0.05$ ; \*\* $p < 0.01$ ; \*\*\* $p < 0.001$

controlling NAFLD development, the lean NAFLD phenotype observed in *Phb1<sup>adipo-/-</sup>* mice may be attributed to alterations of both pathways.

## DISCUSSION

In the current study, we investigated the function of adipocyte PHB1 in the development and progression of NAFLD and uncovered several interesting findings. We demonstrated that mice with adipocyte-specific deletion of *Phb1* displayed a subtype of the lean NAFLD phenotype with low adipose fat mass and severe liver

steatosis under an HFD. Although liver steatosis in *Phb1<sup>adipo-/-</sup>* mice was severe, liver inflammation and fibrosis were comparable to WT mice. Our study further revealed several potential molecular mechanisms that can be attributed to the lean NAFLD phenotype in HFD-fed *Phb1<sup>adipo-/-</sup>* mice, as summarized in Figure 8.

Adipose tissue plays an important role in controlling whole-body energy homeostasis.<sup>[2]</sup> It can store fat for future energy use and also prevent harmful effects of excess fat accumulation in other tissues, such as the liver.<sup>[24]</sup> Several studies have suggested that fat tissue loss leads to an excess of lipid overflow to the liver, resulting in liver steatosis. For example, fat-specific

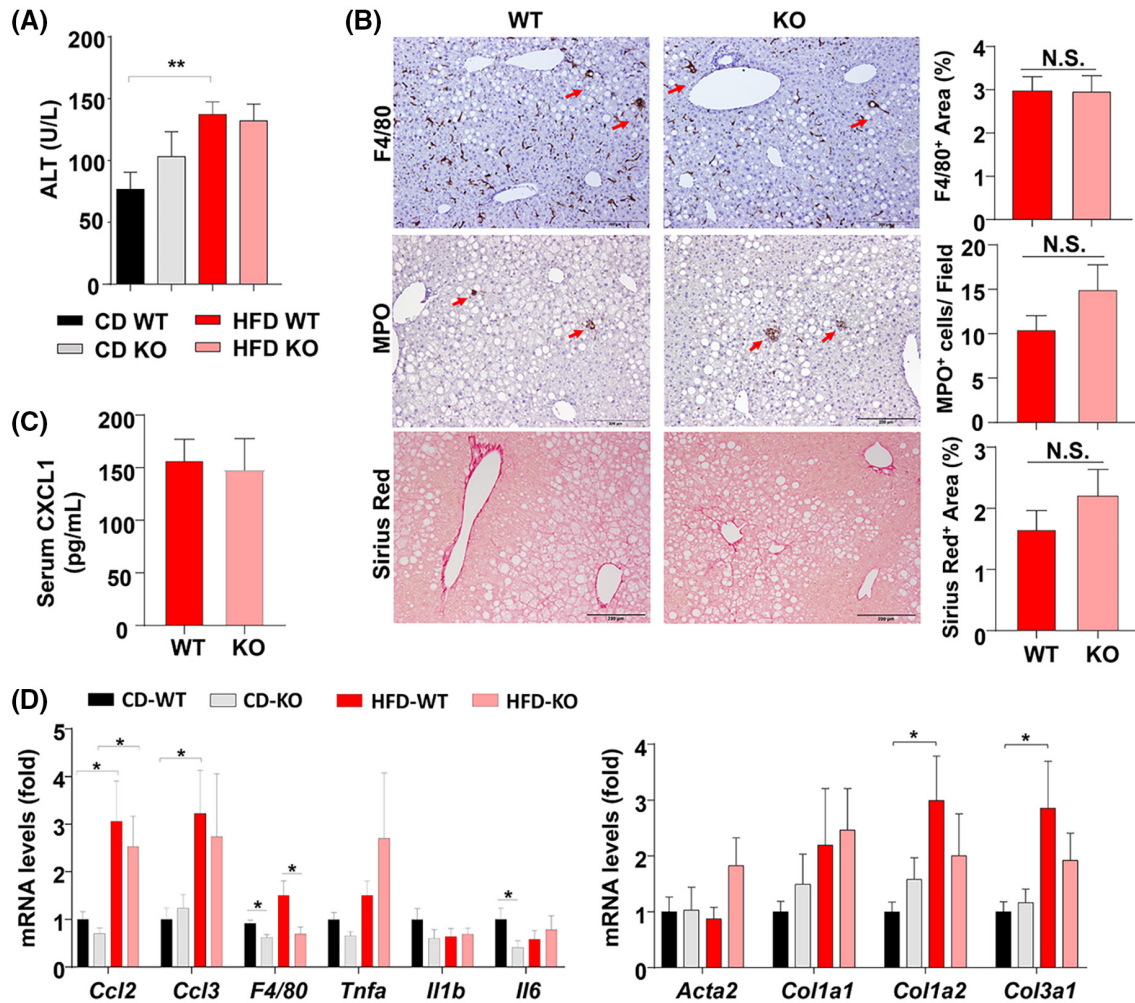


**FIGURE 6** Comparisons of NASH-related liver injury between WT and *Phb1<sup>adipo-/-</sup>* mice. WT and *Phb1<sup>adipo-/-</sup>* mice were fed a chow diet or an HFD for 3 months. (A) Serum ALT levels were measured. (B) Liver sections were subjected to F4/80, MPO, and sirius red staining (scale bars, 200  $\mu$ m). The areas positive for F4/80 and sirius red staining in the liver sections were quantified. The number of MPO<sup>+</sup> cells was counted. (C) Serum levels of CXCL1 in HFD-fed WT and *Phb1<sup>adipo-/-</sup>* mice. (D) Quantitative reverse-transcription polymerase chain reaction analyses of inflammatory mediators and fibrogenic genes. Values represent mean  $\pm$  SEM. Acta2, actin alpha 2, smooth muscle; adipo, adipocyte specific; ALT, alanine aminotransferase; Ccl, C-C motif chemokine ligand; CD, chow diet; Col1 $\alpha$ , collagen type I alpha; CXCL1, chemokine C-X-C motif chemokine ligand 1; HFD, high-fat diet; Il, interleukin; KO, knockout; MPO, myeloperoxidase; mRNA, messenger RNA; NASH, nonalcoholic steatohepatitis; N.S., not significant; PHB1, prohibitin-1; Tnfa, tumor necrosis factor  $\alpha$ ; WT, wild type. \* $p < 0.05$ ; \*\* $p < 0.01$

protein 27 (Fsp27) is responsible for lipid droplet formation in adipocytes. Mice with adipocyte-specific deletion of *Fsp27* were resistant to HFD-induced obesity but presented with marked hepatosteatosis and elevated ALT levels.<sup>[25]</sup> Moreover, adipose-specific *Ppar* knockout mice led to lipodystrophy and develop fatty liver under a chow diet.<sup>[26]</sup> In our study, the adipose tissue mass was dramatically decreased in *Phb1<sup>adipo-/-</sup>* mice compared with WT mice. The reduced fat mass in *Phb1<sup>adipo-/-</sup>* mice was consistent with a previous report.<sup>[14]</sup> In addition, we found decreased expression of genes responsible for lipid droplet formation, such as *Dgat1* and *Plin1*, in *Phb1<sup>adipo-/-</sup>* mice compared to WT mice, and this may contribute to decreased adipose tissue mass and reduced size of adipocytes in these *Phb1<sup>adipo-/-</sup>* mice. It is reasonable to speculate that the limited volume of adipose tissue leads to excess FFA

overflow into liver, which is responsible for the severe hepatic steatosis in *Phb1<sup>adipo-/-</sup>* mice. In addition, our data showed that HFD feeding decreased PHB1 protein expression in adipose tissue, which might contribute to the development of fatty liver by attenuating the adipocyte storage function. Interestingly, HFD feeding did not reduce *Phb1* mRNA but instead slightly increased it in adipose tissue. These results suggest that the expression of PHB1 is regulated at posttranslational levels in adipose tissue. PHB1 has been reported to undergo several posttranslational modifications, including phosphorylation, ubiquitination, and cysteine oxidation.<sup>[27]</sup> For example, PHB1 protein expression level can be up-regulated by long-palate, lung, and nasal epithelium clone 1 (LPLUNC1), which stabilizes PHB1 by inhibiting PHB1 ubiquitination.<sup>[28]</sup> The posttranslational modification of PHB1 in adipose tissue has not been well

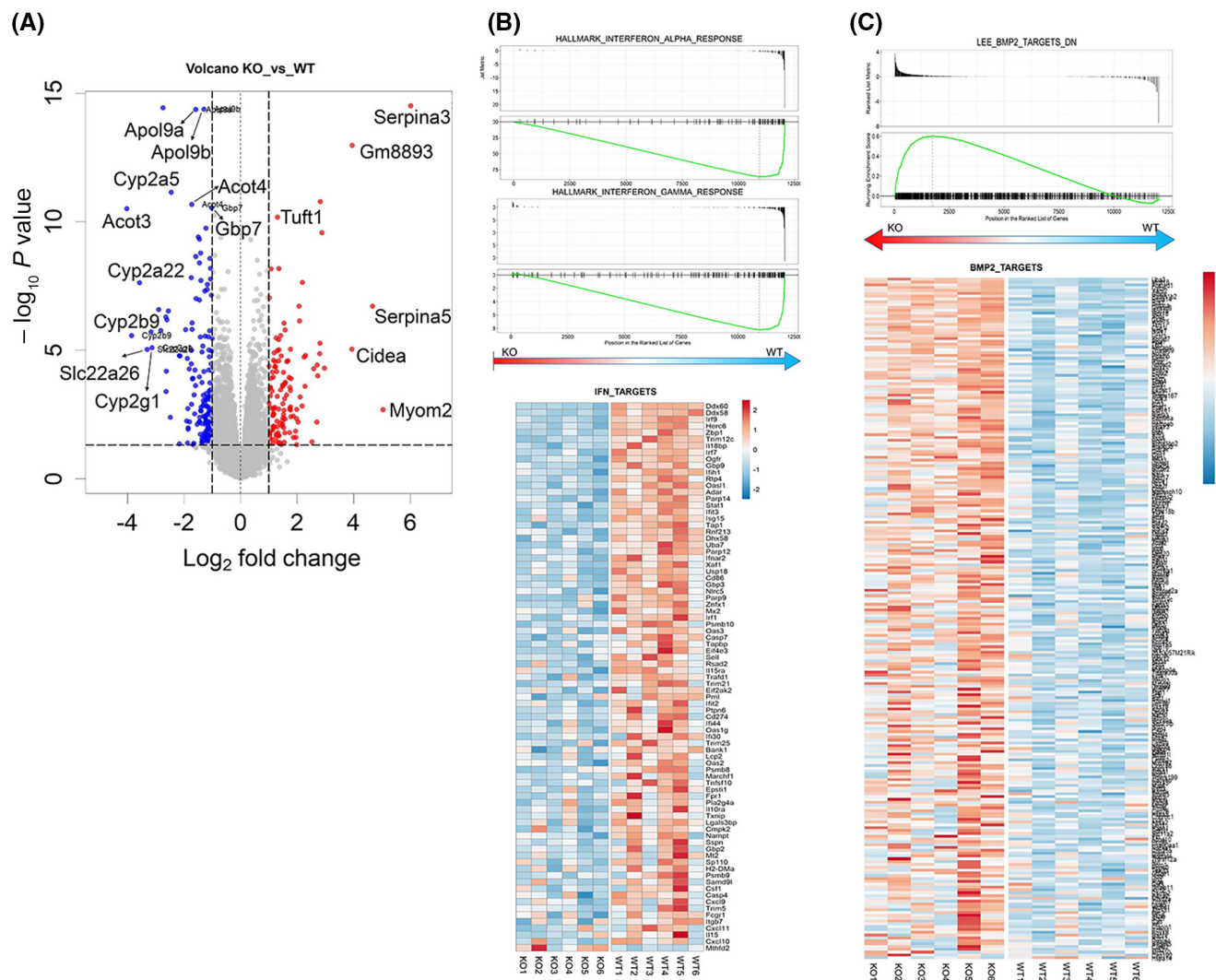


**FIGURE 7** IFN pathway and BMP2 pathway are involved in the pathogenesis of fatty liver in *Phb1<sup>adipo-/-</sup>* mice. WT and *Phb1<sup>adipo-/-</sup>* mice were fed a chow diet or an HFD for 3 months, and liver tissue was subjected to RNA sequencing analysis. (A) Volcano plot of differentially expressed genes in the liver of WT and *Phb1<sup>adipo-/-</sup>* mice. The x axis specifies the  $\log_2$  FCs, and the y axis specifies the  $-\log_{10} p$  value (KO compared to WT). Blue dots represent down-regulated genes ( $\log_2[\text{FC}] < -1$  and  $p < 0.05$ ), and red dots represent up-regulated genes ( $\log_2[\text{FC}] > 1$  and  $p < 0.05$ ). (B) GSEA and heatmap of IFN pathway-related genes. (C) GSEA and heatmap of BMP2-related genes: Acot3, acyl-coenzyme A thioesterase 3; adipo, adipocyte specific; Apol9, apolipoprotein L 9; BMP2, bone morphogenetic protein 2; Cidea, cell death-inducing DFFA like effector A; Cyp, cytochrome P450; FC, fold change; Gbp7, guanylate binding protein 7; Gm8893, predicted gene 8893; GSEA, gene set enrichment analysis; HFD, high-fat diet; IFN, interferon; KO, knockout; Myom2, myomesin 2; PHB1, prohibitin-1; Serpina, serpin family A; Slc22, solute carrier family 22; Tuft1, tuftelin 1; WT, wild type

studied. It will be interesting to explore the mechanisms that regulate PHB1 at the transcriptional, posttranscriptional, and posttranslational levels in adipose tissue in the future.

Although NAFLD is usually associated with obesity, it has recently been recognized that people who are not obese can also develop NAFLD; this is known as “lean NAFLD.”<sup>[29]</sup> The global prevalence of lean NAFLD is approximately 5.1%, which accounts for 19.2% of the NAFLD population.<sup>[29]</sup> Accumulating evidence suggests that lean NAFLD can progress to advanced liver disease in the absence of overweight/obesity.<sup>[30]</sup> There is growing interest in understanding the mechanisms underlying lean NAFLD pathogenesis; however, the

natural history of lean NAFLD has not been characterized, and there are no accepted animal models for lean NAFLD. Patients with lean NAFLD are suggested to have accelerated liver progression and worse mortality<sup>[31]</sup>; yet, other studies suggest that patients with lean NAFLD tend to have less severe liver histologic features and better outcomes.<sup>[30,32]</sup> These controversial data are probably due to the difficulty in selecting proper NAFLD controls for comparison.

Lean NAFLD is defined as NAFLD that develops in patients with a body mass index (BMI)  $< 25 \text{ kg/m}^2$  or BMI  $< 23 \text{ kg/m}^2$  for Asians.<sup>[33]</sup> Even though the pathogenesis of lean NAFLD is not fully understood, some major factors likely contribute to fat accumulation in

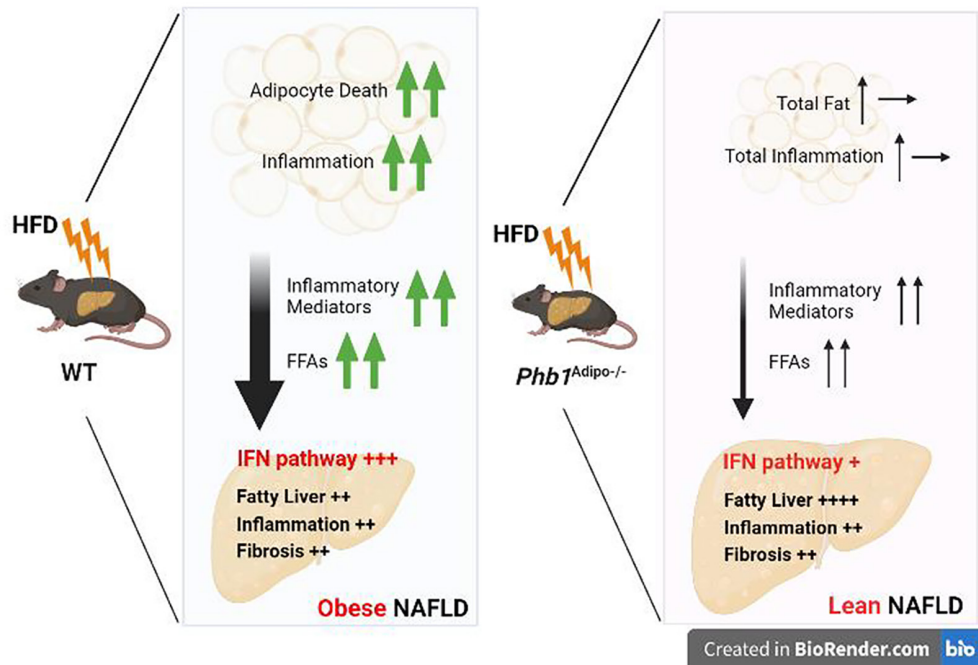


**FIGURE 8** Schematic illustration of the proposed role of adipocyte PHB1 in HFD-induced NAFLD. In WT mice, HFD feeding induces obesity, adipose tissue expansion, and an excess flow of free fatty acids arising from adipose tissue into the liver. Adipose tissue expansion causes adipocyte death and inflammation, exposing the liver to inflammatory mediators and leading to obese NAFLD development. In *Phb1<sup>adipo-/-</sup>* mice, adipose tissue mass is not increased by HFD feeding causing more fat deposition in the liver and severe steatosis. The low fat mass in *Phb1<sup>adipo-/-</sup>* mice results in markedly reduced inflammatory mediators produced from the total adipose tissue, which might be responsible for the comparable liver inflammation and injury in *Phb1<sup>adipo-/-</sup>* mice despite the much more severe steatosis compared to WT mice. Our study suggested that *Phb1<sup>adipo-/-</sup>* mice might represent a subtype of lean NAFLD. *adipo*, adipocyte specific; FFA, free fatty acid; HFD, high-fat diet; IFN, interferon; NAFLD, nonalcoholic fatty liver disease; PHB1, prohibitin-1; WT, wild type. Created in BioRender.com

the liver in patients with lean NAFLD, including genetic predisposition, fat distribution, and metabolic dysfunction.<sup>[34]</sup> Due to the diverse underlying etiologies that contribute to the development of lean NAFLD, lean NAFLD probably includes several subtypes. Vilarinho et al.<sup>[35]</sup> proposed two major subtypes of lean NAFLD, referred to as type 1 (individuals who have visceral adiposity and insulin resistance but normal BMI) and type 2 (individuals in which hepatic steatosis results from a monogenic disorder and therefore with rare genetic variants driving disease). According to this classification, patients with selective loss of adipose tissues due to lipodystrophy belong to type 2 lean NAFLD.<sup>[35]</sup> Our study demonstrated that mice with adipocyte-specific deletion of *Phb1* displayed a phenotype with low fat mass and severe liver steatosis under an HFD, representing a subtype of lean NAFLD in patients; this may be a useful mouse model to study the pathogenesis of a subtype of lean NAFLD.

Severe steatosis is expected to induce more liver injury and inflammation; interestingly, although liver steatosis in *Phb1<sup>adipo-/-</sup>* mice was severe in our study, liver inflammation and fibrosis were mild and similar to WT mice under the HFD. It is well known that TG accumulation in the liver in response to excess FFA overflow is one characteristic of NAFLD that has been considered

historically as the “first hit” in NAFLD development.<sup>[36]</sup> The mechanisms underlying the shift from hepatic steatosis into NASH remain incompletely understood. Several studies have suggested the different roles of specific lipid types in liver damage, inflammation, and hepatocyte apoptosis. For example, evidence indicated that saturated fatty acids (SFAs) are potentially cytotoxic by triggering apoptosis. SCD1, the enzyme that converts SFAs to monounsaturated fatty acids (MUFAs) exhibits a protective effect against SFA lipotoxicity.<sup>[37]</sup> A previous study found that genetic or pharmacologic inhibition of SCD1 sensitized hepatocytes to apoptosis and that SCD1 knockout mice accumulated less TGs but showed increased hepatocyte apoptosis and liver injury under a methionine- and choline-deficient diet.<sup>[38]</sup> In our study, the hepatic expression of SCD1 was significantly increased in *Phb1<sup>adipo-/-</sup>* mice; this might result in a trend toward MUFA formation, leading to liver adaptation and benign liver steatosis. In addition, the dramatically decreased fat mass in *Phb1<sup>adipo-/-</sup>* mice may lead to reduced FFA flow from adipose tissue into the liver, which may be responsible for altered lipid compartmentation in the liver of *Phb1<sup>adipo-/-</sup>* mice. It will be interesting to analyze lipid compartmentation, particularly the ratio of monounsaturated to saturated FFAs in the liver of *Phb1<sup>adipo-/-</sup>* mice in the future.

It is well accepted that adipose tissue inflammation plays an important role in promoting NASH.<sup>[39]</sup> Adipose tissue expansion in obesity causes hypoxia, inflammation, and subsequent adipocyte death, which triggers chronic and low-grade inflammation, exposing liver tissue to inflammatory cytokines that cause secondary inflammation in the liver.<sup>[39]</sup> Our previous study suggested that adipocyte death causes hepatocyte injury and inflammation in the liver and accelerates NASH progression.<sup>[40]</sup> In our study, inflammatory cell numbers and gene expression levels of inflammatory mediators in adipose tissue were similar between WT and *Phb1*<sup>adipo<sup>-/-</sup></sup> mice when the same amount of adipose tissues were compared; however, because of the dramatically reduced adipose tissue mass, HFD-fed *Phb1*<sup>adipo<sup>-/-</sup></sup> mice had markedly lower levels of total adipose tissue inflammation than HFD-fed WT mice. Thus, we speculate that *Phb1* adipocyte deficiency led to reduced production of proinflammatory mediators from adipose tissue, thereby protecting liver from developing liver inflammation and fibrosis, despite severe liver steatosis.

Adipose tissue may also affect NAFLD progression by secreting adipokines, such as leptin and adiponectin. In patients with lipodystrophy, leptin treatment was found to improve insulin sensitivity and reduce hepatic TG content.<sup>[41]</sup> Profibrogenic activities of leptin in liver have also been reported.<sup>[42]</sup> For example, an animal model with leptin deficiency, such as obese (ob)/ob mice and leptin-resistant rats, do not develop liver fibrosis.<sup>[42]</sup> Rotundo et al.<sup>[43]</sup> have reported that serum levels of leptin are significantly higher in patients with NAFLD with higher BMI. Interestingly, leptin levels were positively related to the severity of liver fibrosis in classic NAFLD but not in lean NAFLD, suggesting that the lower leptin levels in individuals with lean NAFLD may not be able to accelerate liver fibrosis. In our study, we did not observe significantly increased liver fibrosis in *Phb1*<sup>adipo<sup>-/-</sup></sup> mice despite their marked increased liver steatosis. Our data showed that the lower serum levels of leptin in *Phb1*<sup>adipo<sup>-/-</sup></sup> mice may contribute to slow liver fibrosis progression. Apart from leptin, adipose tissue secretes various adipokines into circulation that are involved in the pathogenesis of NAFLD. For example, S100A8/A9<sup>[44]</sup> and secreted protein acidic and rich in cysteine-like protein 1 (SPARCL1),<sup>[45]</sup> which are generated from adipose tissue, have been reported to drive the progression from liver steatosis to NASH. Although we have not measured these adipokines and inflammatory mediators in our study, we speculate that the abnormal adipose tissue function in *Phb1*<sup>adipo<sup>-/-</sup></sup> mice might lead to the alteration of adipokines and thus regulate NAFLD progression. Measurement of adipokines is needed to explore the differences in the adipokines generated from WT and *Phb1*<sup>adipo<sup>-/-</sup></sup> mice. It will also be interesting to examine whether treatment of hepatocytes with the supernatants of WT and *Phb1*<sup>adipo<sup>-/-</sup></sup> adipose

tissue extracts will generate different effects on fat metabolism and inflammatory responses in hepatocytes.

Extracellular vehicles (EVs) from adipose tissues have recently been indicated to play an important role in the crosstalk between adipose tissue and liver. For example, adipose tissue macrophage (ATM)-EVs from obese mice containing precursor microRNA (miR)-155 are taken up by hepatocytes, leading to increased insulin resistance by suppressing PPAR $\gamma$ , while treatment of obese mice with ATM-EVs from lean mice improves insulin resistance.<sup>[46]</sup> We speculate that PHB1 deficiency in adipose tissue may result in alteration of the contents of EVs released from adipose tissue that are involved in the regulation of liver function. It will be interesting to further explore the contents of EVs, especially microRNAs, in EVs that are derived from adipose tissue in *Phb1*<sup>adipo<sup>-/-</sup></sup> mice in the future.

Our RNA-seq analyses identified two altered pathways that may explain similar liver inflammation and fibrosis in *Phb1*<sup>adipo<sup>-/-</sup></sup> and WT mice under HFD feeding despite more severe steatosis in the former group. First, the interferon (IFN) pathway is markedly down-regulated in the liver of *Phb1*<sup>adipo<sup>-/-</sup></sup> mice compared to WT mice under HFD feeding. The IFN pathway has been implicated in the development and progression of NAFLD, as supported by both genetic evidence and animal studies. For example, the IFN lambda 4 rs368234815 TT> $\delta$ G variant is associated with severity of fibrosis in patients with NAFLD.<sup>[47]</sup> Deletion of IFN alpha and beta receptor subunit 1 (*Ifnar1*) in hepatocytes worsened liver steatosis and inflammation in mice under a methionine-choline-deficient diet.<sup>[48]</sup> Knocking down of stimulator of IFN genes (STING) resulted in attenuated liver inflammation in NAFLD.<sup>[49]</sup> Thus, the suppressed IFN pathway likely explains mild liver inflammation but severe steatosis in HFD-fed *Phb1*<sup>adipo<sup>-/-</sup></sup> mice. The reasons behind the suppressed IFN pathway in the liver of *Phb1*<sup>adipo<sup>-/-</sup></sup> compared to WT mice remain obscure. Further studies are needed to analyze the serum levels of inflammatory cytokines. Second, the BMP pathway is up-regulated in the liver of *Phb1*<sup>adipo<sup>-/-</sup></sup> mice compared to WT mice under an HFD. BMPs belong to the transforming growth factor beta (TGF- $\beta$ ) family, which plays important roles in liver fibrosis. Hepatic BMP2 is mainly expressed in parenchymal hepatocytes and activated HSCs, and it inhibits TGF- $\beta$ 1-induced HSC activation, thereby reducing liver fibrosis.<sup>[50]</sup> It has been reported that BMP signaling accelerates the development of hepatic steatosis by regulating hepatic DGAT2 expression and activity.<sup>[50]</sup> Thus, we speculated that the up-regulated BMP2 target genes may explain the increased fat content but mild liver fibrosis in the liver of *Phb1*<sup>adipo<sup>-/-</sup></sup> mice. Further studies are needed to explore the mechanisms underlying the functions of the IFN pathway and BMP signaling in regulating lipid metabolism in *Phb1*<sup>adipo<sup>-/-</sup></sup> mice.

## ACKNOWLEDGMENT

None.

## FUNDING INFORMATION

National Institute on Alcohol Abuse and Alcoholism, National Institutes of Health; Grant Number R01DK123763.

## CONFLICTS OF INTEREST

Richard Parker consults for Durect Corporation and received honoraria from Norgine. The other authors have nothing to report.

## ORCID

Richard Parker  <https://orcid.org/0000-0003-4888-8670>

Bin Gao  <https://orcid.org/0000-0002-0505-2972>

## REFERENCES

1. Younossi Z, Tacke F, Arrese M, Chander Sharma B, Mostafa I, Bugianesi E, et al. Global perspectives on nonalcoholic fatty liver disease and nonalcoholic steatohepatitis. *Hepatology*. 2019;69:2672–82.
2. Azzu V, Vacca M, Virtue S, Allison M, Vidal-Puig A. Adipose tissue-liver cross talk in the control of whole-body metabolism: implications in nonalcoholic fatty liver disease. *Gastroenterology*. 2020;158:1899–912.
3. Rodrigues RM, Guan Y, Gao B. Targeting adipose tissue to tackle NASH: SPARCL1 as an emerging player. *J Clin Invest*. 2021;131:e153640.
4. Duval C, Thissen U, Keshtkar S, Accart B, Stienstra R, Boekschoten MV, et al. Adipose tissue dysfunction signals progression of hepatic steatosis towards nonalcoholic steatohepatitis in C57BL/6 mice. *Diabetes*. 2010;59:3181–91.
5. du Plessis J, van Pelt J, Korf H, Mathieu C, van der Schueren B, Lannoo M, et al. Association of adipose tissue inflammation with histologic severity of nonalcoholic fatty liver disease. *Gastroenterology*. 2015;149:635–48.e14.
6. Signorile A, Sgaramella G, Bellomo F, De Rasmio D. Prohibitins: a critical role in mitochondrial functions and implication in diseases. *Cells*. 2019;8:71.
7. Barbier-Torres L, Beraza N, Fernandez-Tussy P, Lopitz-Otsoa F, Fernandez-Ramos D, Zubiete-Franco I, et al. Histone deacetylase 4 promotes cholestatic liver injury in the absence of prohibitin-1. *Hepatology*. 2015;62:1237–48.
8. Fan W, Yang H, Liu T, Wang J, Li TW, Mavila N, et al. Prohibitin 1 suppresses liver cancer tumorigenesis in mice and human hepatocellular and cholangiocarcinoma cells. *Hepatology*. 2017;65:1249–66. Erratum in: *Hepatology*. 2017;66:1708.
9. Ko KS, Tomasi ML, Iglesias-Ara A, French BA, French SW, Ramani K, et al. Liver-specific deletion of prohibitin 1 results in spontaneous liver injury, fibrosis, and hepatocellular carcinoma in mice. *Hepatology*. 2010;52:2096–108.
10. Ande SR, Nguyen KH, Padilla-Meier GP, Wahida W, Nyomba BL, Mishra S. Prohibitin overexpression in adipocytes induces mitochondrial biogenesis, leads to obesity development, and affects glucose homeostasis in a sex-specific manner. *Diabetes*. 2014;63:3734–41.
11. Vessal M, Mishra S, Moulik S, Murphy LJ. Prohibitin attenuates insulin-stimulated glucose and fatty acid oxidation in adipose tissue by inhibition of pyruvate carboxylase. *FEBS J*. 2006;273:568–76.
12. Salameh A, Daquinag AC, Staquicini DI, An Z, Hajjar KA, Pasqualini R, et al. Prohibitin/annexin 2 interaction regulates fatty acid transport in adipose tissue. *JCI Insight*. 2016;1:e86351.
13. Ande SR, Xu Z, Gu Y, Mishra S. Prohibitin has an important role in adipocyte differentiation. *Int J Obes (Lond)*. 2012;36:1236–44.
14. Gao Z, Daquinag AC, Fussell C, Djehal A, Desaubry L, Kolonin MG. Prohibitin inactivation in adipocytes results in reduced lipid metabolism and adaptive thermogenesis impairment. *Diabetes*. 2021;70:2204–12.
15. Ande SR, Nguyen KH, Gregoire Nyomba BL, Mishra S. Prohibitin-induced, obesity-associated insulin resistance and accompanying low-grade inflammation causes NASH and HCC. *Sci Rep*. 2016;6:23608.
16. Bolger AM, Lohse M, Usadel B. Trimmomatic: a flexible trimmer for Illumina sequence data. *Bioinformatics*. 2014;30:2114–20.
17. Kim D, Paggi JM, Park C, Bennett C, Salzberg SL. Graph-based genome alignment and genotyping with HISAT2 and HISAT-genotype. *Nat Biotechnol*. 2019;37:907–15.
18. Liao Y, Smyth GK, Shi W. featureCounts: an efficient general purpose program for assigning sequence reads to genomic features. *Bioinformatics*. 2014;30:923–30.
19. Love MI, Huber W, Anders S. Moderated estimation of fold change and dispersion for RNA-seq data with DESeq2. *Genome Biol*. 2014;15:550.
20. Yu G, Wang L-G, Han Y, He Q-Y. clusterProfiler: an R package for comparing biological themes among gene clusters. *OMICS*. 2012;16:284–7.
21. Troeger JS, Mederacke I, Gwak GY, Dapito DH, Mu X, Hsu CC, et al. Deactivation of hepatic stellate cells during liver fibrosis resolution in mice. *Gastroenterology*. 2012;143:1073–83.e22.
22. Zhou L, Xu L, Ye J, Li D, Wang W, Li X, et al. Cidea promotes hepatic steatosis by sensing dietary fatty acids. *Hepatology*. 2012;56:95–107.
23. Hunt MC, Siponen MI, Alexson SE. The emerging role of acyl-CoA thioesterases and acyltransferases in regulating peroxisomal lipid metabolism. *Biochim Biophys Acta*. 2012;1822:1397–410.
24. Cohen P, Spiegelman BM. Cell biology of fat storage. *Mol Biol Cell*. 2016;27:2523–7.
25. Tanaka N, Takahashi S, Matsubara T, Jiang C, Sakamoto W, Chanturiya T, et al. Adipocyte-specific disruption of fat-specific protein 27 causes hepatosteatosis and insulin resistance in high-fat diet-fed mice. *J Biol Chem*. 2015;290:3092–105.
26. He W, Barak Y, Hevener A, Olson P, Liao D, Le J, et al. Adipose-specific peroxisome proliferator-activated receptor gamma knockout causes insulin resistance in fat and liver but not in muscle. *Proc Natl Acad Sci U S A*. 2003;100:15712–7.
27. Barbier-Torres L, Lu SC. Prohibitin 1 in liver injury and cancer. *Exp Biol Med (Maywood)*. 2020;245:385–94.
28. Wang H, Zhou Y, Oyang L, Han Y, Xia L, Lin J, et al. LPLUNC1 stabilises PHB1 by counteracting TRIM21-mediated ubiquitination to inhibit NF-kappaB activity in nasopharyngeal carcinoma. *Oncogene*. 2019;38:5062–75.
29. Ye Q, Zou B, Yeo YH, Li J, Huang DQ, Wu Y, et al. Global prevalence, incidence, and outcomes of non-obese or lean non-alcoholic fatty liver disease: a systematic review and meta-analysis. *Lancet Gastroenterol Hepatol*. 2020;5:739–52.
30. Younes R, Govaere O, Petta S, Miele L, Tiniakos D, Burt A, et al. Caucasian lean subjects with non-alcoholic fatty liver disease share long-term prognosis of non-lean: time for reappraisal of BMI-driven approach? *Gut*. 2022;71:382–90.
31. Zou B, Yeo YH, Nguyen VH, Cheung R, Ingelsson E, Nguyen MH. Prevalence, characteristics and mortality outcomes of obese, nonobese and lean NAFLD in the United States, 1999–2016. *J Intern Med*. 2020;288:139–51.
32. Leung JC, Loong TC, Wei JL, Wong GL, Chan AW, Choi PC, et al. Histological severity and clinical outcomes of nonalcoholic fatty liver disease in nonobese patients. *Hepatology*. 2017;65:54–64.

33. Younes R, Bugianesi E. NASH in lean individuals. *Semin Liver Dis.* 2019;39:86–95.
34. Ahadi M, Molooghi K, Masoudifar N, Namdar AB, Vossoughinia H, Farzanehfard M. A review of non-alcoholic fatty liver disease in non-obese and lean individuals. *J Gastroenterol Hepatol.* 2021;36:1497–507.
35. Vilarinho S, Ajmera V, Zheng M, Loomba R. Emerging role of genomic analysis in clinical evaluation of lean individuals With NAFLD. *Hepatology.* 2021;74:2241–50.
36. Day CP, James OF. Steatohepatitis: a tale of two "hits"? *Gastroenterology.* 1998;114:842–5.
37. Ravaut G, Legiot A, Bergeron KF, Mounier C. Monounsaturated fatty acids in obesity-related inflammation. *Int J Mol Sci.* 2020;22:330.
38. Alkhourri N, Dixon LJ, Feldstein AE. Lipotoxicity in nonalcoholic fatty liver disease: not all lipids are created equal. *Expert Rev Gastroenterol Hepatol.* 2009;3:445–51.
39. Rosso C, Kazankov K, Younes R, Esmaili S, Marietti M, Sacco M, et al. Crosstalk between adipose tissue insulin resistance and liver macrophages in non-alcoholic fatty liver disease. *J Hepatol.* 2019;71:1012–21.
40. Kim SJ, Feng D, Guillot A, Dai S, Liu F, Hwang S, et al. Adipocyte death preferentially induces liver injury and inflammation through the activation of chemokine (C-C motif) receptor 2-positive macrophages and lipolysis. *Hepatology.* 2019;69:1965–82.
41. Petersen KF, Oral EA, Dufour S, Befroy D, Ariyan C, Yu C, et al. Leptin reverses insulin resistance and hepatic steatosis in patients with severe lipodystrophy. *J Clin Invest.* 2002;109:1345–50.
42. Leclercq IA, Farrell GC, Schriemer R, Robertson GR. Leptin is essential for the hepatic fibrogenic response to chronic liver injury. *J Hepatol.* 2002;37:206–13.
43. Rotundo L, Persaud A, Feurdean M, Ahlawat S, Kim HS. The Association of leptin with severity of non-alcoholic fatty liver disease: a population-based study. *Clin Mol Hepatol.* 2018;24:392–401.
44. Rodrigues RM, He Y, Hwang S, Bertola A, Mackowiak B, Ahmed YA, et al. E-selectin-dependent inflammation and lipolysis in adipose tissue exacerbate steatosis-to-NASH progression via S100A8/9. *Cell Mol Gastroenterol Hepatol.* 2022;13:151–71.
45. Liu B, Xiang L, Ji J, Liu W, Chen Y, Xia M, et al. Sparcl1 promotes nonalcoholic steatohepatitis progression in mice through upregulation of CCL2. *J Clin Invest.* 2021;131:e144801.
46. Ying W, Riopel M, Bandyopadhyay G, Dong Y, Birmingham A, Seo JB, et al. Adipose tissue macrophage-derived exosomal miRNAs can modulate in vivo and in vitro insulin sensitivity. *Cell.* 2017;171:372–84.e312.
47. Petta S, Valenti L, Tuttolomondo A, Dongiovanni P, Pipitone RM, Camma C, et al. Interferon lambda 4 rs368234815 TT>δG variant is associated with liver damage in patients with nonalcoholic fatty liver disease. *Hepatology.* 2017;66:1885–93.
48. Wieser V, Adolph TE, Grander C, Grabherr F, Enrich B, Moser P, et al. Adipose type I interferon signalling protects against metabolic dysfunction. *Gut.* 2018;67:157–65.
49. Qiao JT, Cui C, Qing L, Wang LS, He TY, Yan F, et al. Activation of the STING-IRF3 pathway promotes hepatocyte inflammation, apoptosis and induces metabolic disorders in nonalcoholic fatty liver disease. *Metabolism.* 2018;81:13–24.
50. Thayer TE, Lino Cardenas CL, Martyn T, Nicholson CJ, Traeger L, Wunderer F, et al. The role of bone morphogenetic protein signaling in non-alcoholic fatty liver disease. *Sci Rep.* 2020;10:9831.

## SUPPORTING INFORMATION

Additional supporting information can be found online in the Supporting Information section at the end of this article.

**How to cite this article:** Wang X, Kim S-J, Guan Y, Parker R, Rodrigues RM, Feng D, et al. Deletion of adipocyte prohibitin 1 exacerbates high-fat diet-induced steatosis but not liver inflammation and fibrosis. *Hepatol Commun.* 2022;6:3335–3348. <https://doi.org/10.1002/hep4.2092>